DE GRUYTER OPEN
Studia Geotechnica et Mechanica, Vol. XXXVI, No. 4, 2014
DOI: 10.2478/sgem-2014-0035

X-RAY MICROTOMOGRAPHY (μCT) AS A USEFUL TOOL FOR VISUALIZATION AND INTERPRETATION OF SHEAR STRENGTH TEST RESULTS

DAMIAN STEFANIUK, MATYLDA TANKIEWICZ, JOANNA STRÓŻYK

Institute of Geotechnics and Hydrotechnics, Wrocław University of Technology

Abstract: The paper demonstrates the applicability of X-ray microtomography (μCT) to analysis of the results of shear strength examinations of clayey soils. The method of X-ray three-dimensional imaging offers new possibilities in soil testing. The work focuses on a non-destructive method of evaluation of specimen quality used in shear tests and mechanical behavior of soil. The paper presents the results of examination of 4 selected clayey soils. Specimens prepared for the triaxial test have been scanned using μCT before and after the triaxial compression tests. The shear strength parameters of the soils have been estimated. Changes in soil structure caused by compression and shear failure have been presented as visualizations of the samples tested. This allowed for improved interpretation and evaluation of soil strength parameters and recognition of pre-existing fissures and the exact mode of failure. Basic geometrical parameters have been determined for selected cross-sections of specimens after failure. The test results indicate the utility of the method applied in soil testing.

Key words: *X-ray microtomography, shear strength, shear plane, fine-grained soil, triaxial test*

1. INTRODUCTION

X-ray-computed tomography is a rapidly evolving technology that allows a non-destructive measurement and visualization of internal structure of scanned objects. This technique yields three-dimensional images that can be measured and modified. However, its applicability to geotechnical problems and soil science is only beginning to be explored. The technique enables pore structure, discontinuities, or other defects to be recognized in the soil without destroying the specimen. Using this method we can recognize with good accuracy the pre-existing fissures or cracks and density changes that may affect the mechanical behavior of the soil before commencing tests. This is particularly important in the cases of (a) shear strength tests, where the intact test sample plays an important role in interpreting the results; and (b) high-value samples (taken from a great depth) of limited availability, where the structure is heavily disturbed by the enormous changes in the stress associated with drilling and sampling.

In the standard approach to soil-strength examination one is not required to investigate the structure of the specimen before the test. However, omission of this part may implicate invalid interpretations of test results. Exact recognition of shear plane may increase understanding of mechanical behavior of soil. The paper presents results of an examination of specimens before and after triaxial compression tests with X-ray microtomography. The examination was carried out on four selected samples of fine-grained clayey soil taken from great depth.

2. X-RAY MICROTOMOGRAPHY

X-ray-computed tomography is a three-dimensional imaging technique that uses a series of radiographic images to reconstruct a map of an object's X-ray absorption [1]. It was originally developed for medical purposes, but it was quickly adapted to other scientific fields like engineering and geology.

A beam of X-rays is characterized by its photon flux density, or intensity, and spectral energy distribution. When a beam of X-rays passes through a material, the object itself becomes a source of secondary X-rays and electrons. Because of these secondary processes, a portion of the primary beam is absorbed or scattered out of the beam. For monochromatic radiation, to relate the intensity of transmitted radiation I and the intensity of incident radiation I_0, Lambert–Beer's law is used

$$I = I_0 e^{-\mu D} \quad (1)$$

where D is the distance traveled through the material and μ is the attenuation coefficient of the material that depends on the electron density, the energy of the radiation, and the bulk density of the material [13]. The images produced by tomographic scans and subsequent reconstruction consist in gray scale volumes where the pixel intensity is roughly proportional to the object's density.

Application of computed tomography yields the best results for materials that are marked by differences in density, with the highest contrast being between solids and atmosphere. This technique is therefore often used in soil science to determine pore network and porosity of soils [6], 12]. It is also used, among other applications, to recognize the distribution of bulk density or water content and changes in structure [9]. Investigations into the mechanics of behavior of soils are conducted during triaxial compression [4], [15]. However, those types of tests are performed on much smaller samples than in standard triaxial tests, so this technique can be applied only to quite homogenous soils. Another approach is to perform the standard triaxial test and scan the sample afterwards [14].

In general, computed tomography scanners can be assigned to one of four groups based on their spatial resolution and the size of the scanned object. The classification, proposed in [7], is provided in Table 1. Unlike conventional computed tomography, microtomography (μCT) achieves a much higher spatial resolution by combining extremely bright, monochromatic synchrotron radiation with high-quality optics and X-ray detection. For purposes of this paper the entire examination was done using a SkyScan1172 high-resolution μCT. The maximum object size for this scanner is 27 mm in diameter for a single scan and 50 mm in diameter for an offset scan. At the maximum setting, the focal spot size is about 0.5 μm. The tube voltage in this instrument can be set from 20 to 100 kV, and the X-ray tube source is closed with the maximum power of 10 V [11]. A schematic illustration of the μCT system used is given in Fig. 1.

Table 1. General classification of computed tomography [7]

Type	Scale of observation	Scale of resolution
Conventional	m	1 mm
High-resolution	dm	100 μm
Ultra-high-resolution	cm	10 μm
Microtomography	mm	1 μm

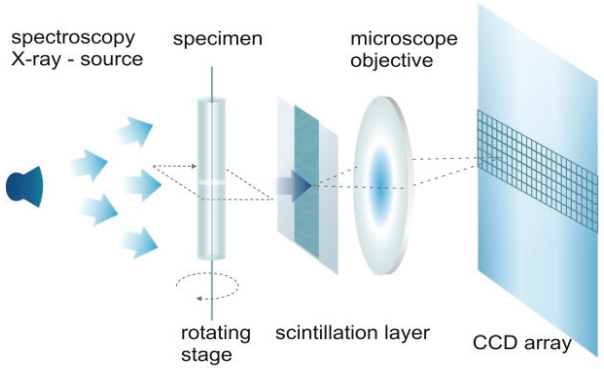

Fig. 1. Schematic illustration of a microtomography system [3]

3. MATERIALS AND METHODS

Laboratory examinations were conducted on four selected samples of fine-grained, strongly consolidated soils from Lower Silesia. The samples were taken from a depth of about 300 m below ground level. Test samples were silty clay (2 samples), clay (1 sample) and clayey silt (1 sample) with some portions of organic matter (C_{om} about 7%, except A2 sample with C_{om} = 20%). The basic information about the soils investigated is summarized in Table 2. The soil symbol and the consistency have been determined according to ISO [10].

Table 2. Basic soil sample properties

Sample	Soil symbol	Consistency	Averaged vertical stress *in situ* [MPa]	Bulk density ρ [g/cm^3]	Water content w [%]	Organic matter content C_{om} [%]
A1	clSi+Or	stiff	4.3	1.76	35.1	7.9
A2	Cl+Or	very stiff	6.3	1.63	46.8	20.0
A4	siCl+Or	stiff	6.6	2.13	18.7	7.2
B9	Cl+Or	very stiff	4.6	1.98	23.4	7.8

The investigations were carried out in three stages. First, the specimens, prepared for the triaxial test, were scanned in the μCT. Next, triaxial tests TXCIU were executed. Finally, after failure in the triaxial apparatus, specimens were scanned once again.

The triaxial tests were done on a triaxial system by ELE International Ltd. Each of the intact soil specimens, 38 mm in diameter and 76 mm in height, was trimmed from cylindrical core samples. Each test was carried out according to a procedure called TXCIU (reconsolidated, undrained) [5]. In order to estimate soil strength parameters ϕ' (effective friction angle) and c' (effective cohesion), three specimens of each type of soil were tested in the triaxial apparatus with confining pressures of σ_3 = 200 kPa, 400 kPa, and 600 kPa. At the first stage of the test, soil was consolidated following application of isotropic confining pressure. At the second stage, each specimen was subjected to undrained confined compression. The speed of compression was 2.4 mm/min, with pore water pressure under observation.

The X-ray scanning procedure was conducted with the SkyScan 1172 high-resolution μCT. Tube voltage, exposure time, and rotation step were 80 kV, 660 ms and 0,3°, respectively. An Al + Cu filter, 0.7 mm thick, was applied. The image matrix is 1740 × 1740 pixels with a slice thickness of 27 μm. The main results of the tests are comprised by pairs of scans of specimens – before and after the TXCIU test conducted with confining pressure σ_3 = 600 kPa and some examples of possible basic measurement.

4. RESULTS

The test results are presented in Figs. 2–14 and in Tables 3 and 4. Figures 2, 5, 8, 11 show the images of

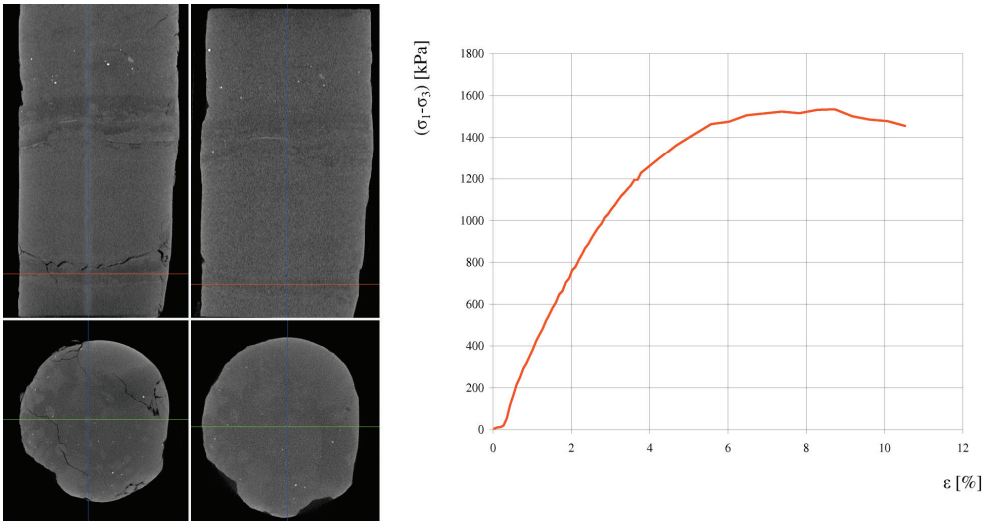

Fig. 2. Images of sample A1 before (left) and after (right) the test; stress-strain curve for σ_3 = 600 kPa

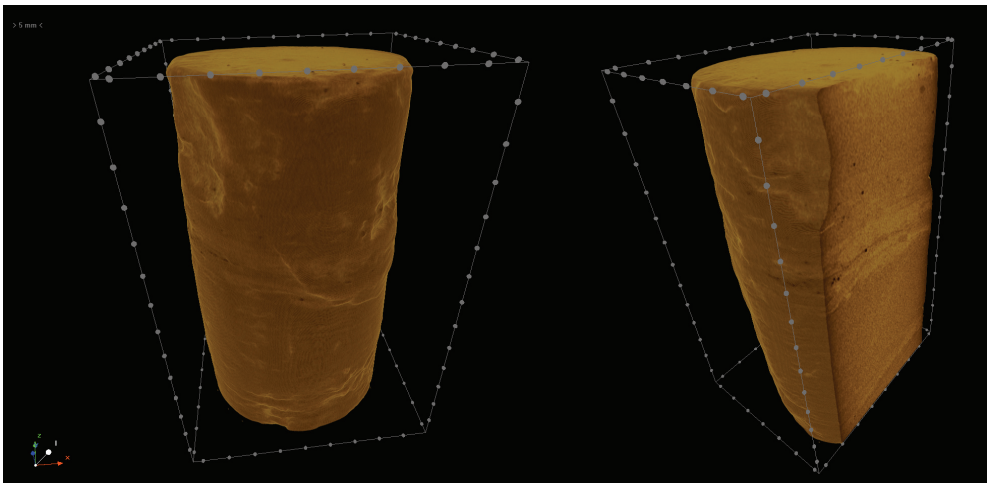

Fig. 3. 3D visualizations of sample A1

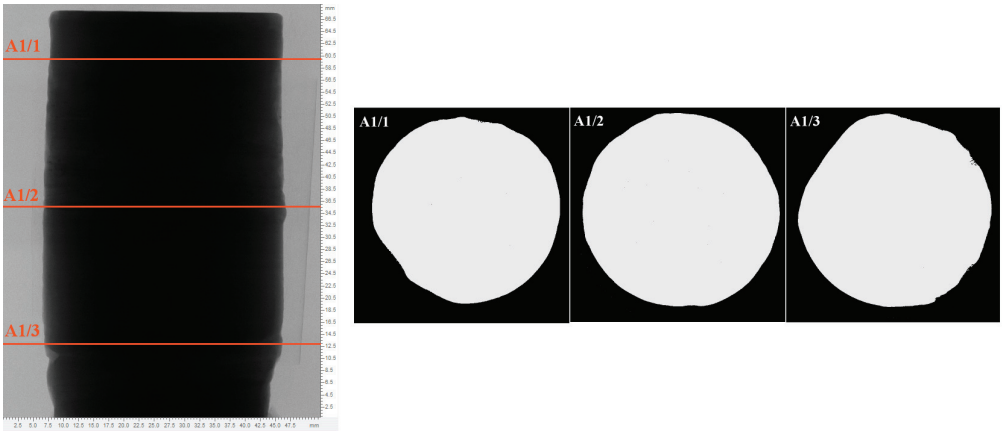

Fig. 4. Selected cross-sections of sample A1 after the triaxial test

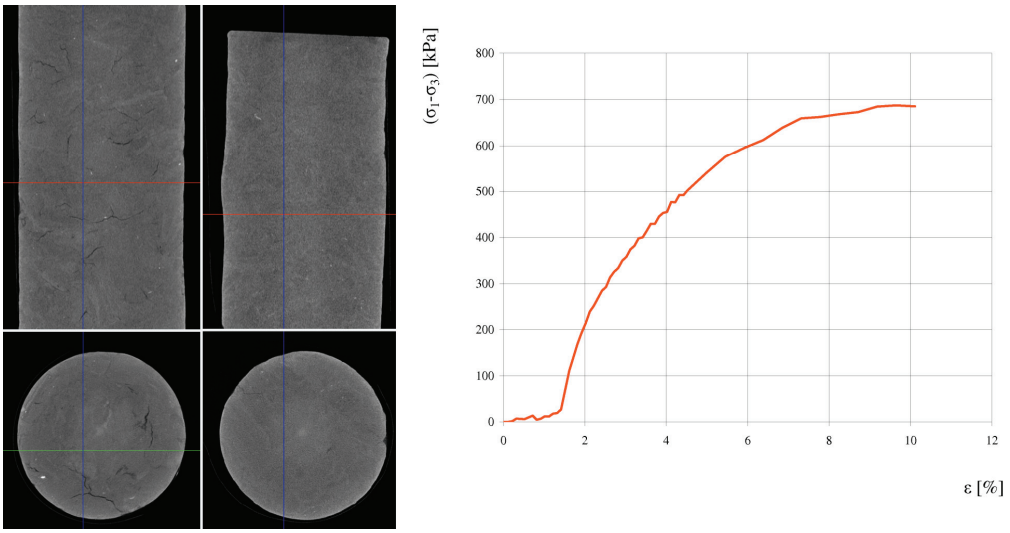

Fig. 5. Images of sample A2 before (left) and after (right) the test; stress-strain curve for σ_3 = 600 kPa

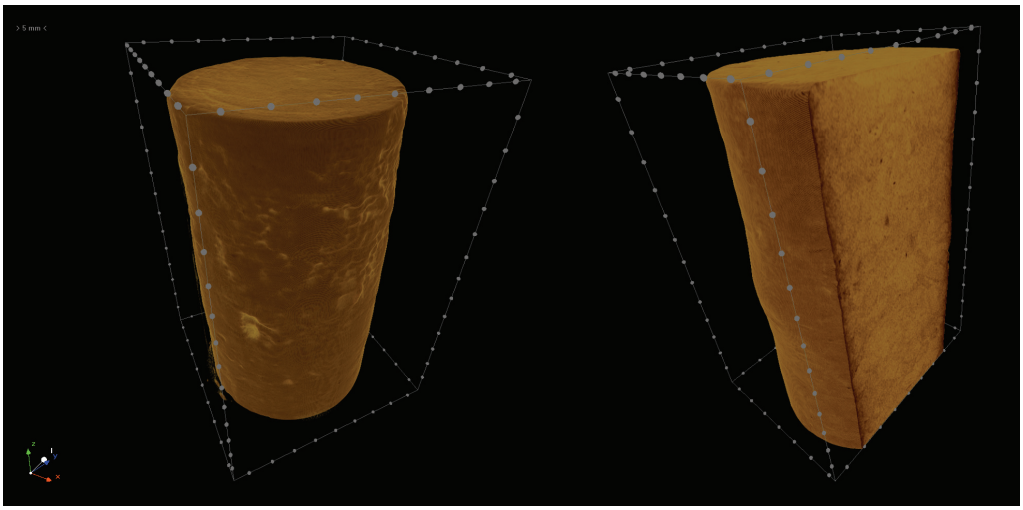

Fig. 6. 3D visualizations of sample A2

specimens before and after triaxial compression with σ_3 = 600 kPa and corresponding deviatoric stress-axial strain curves. Figures 3, 6, 9, 12 comprise depictions of the three-dimensional nature of data and present post-failure visualizations of the specimens. Figures 4, 7, 10, 13 provide selected cross-sections of specimens

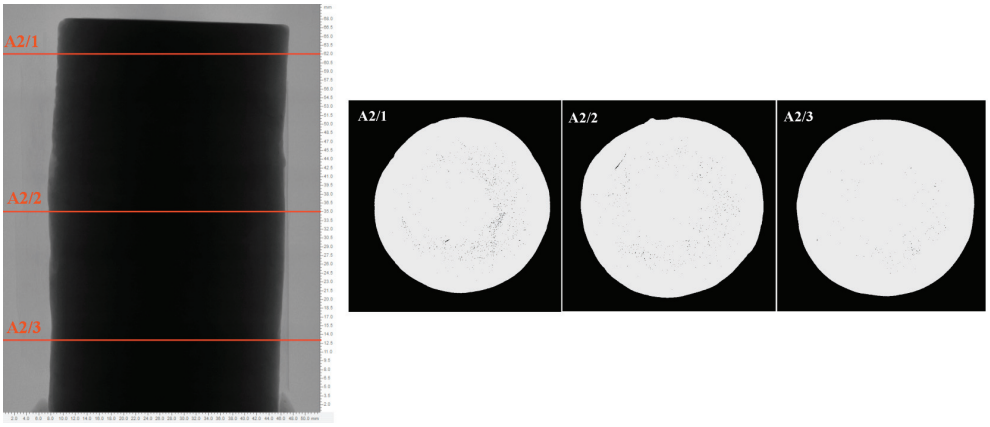

Fig. 7. Selected cross-sections of sample A2 after the triaxial test

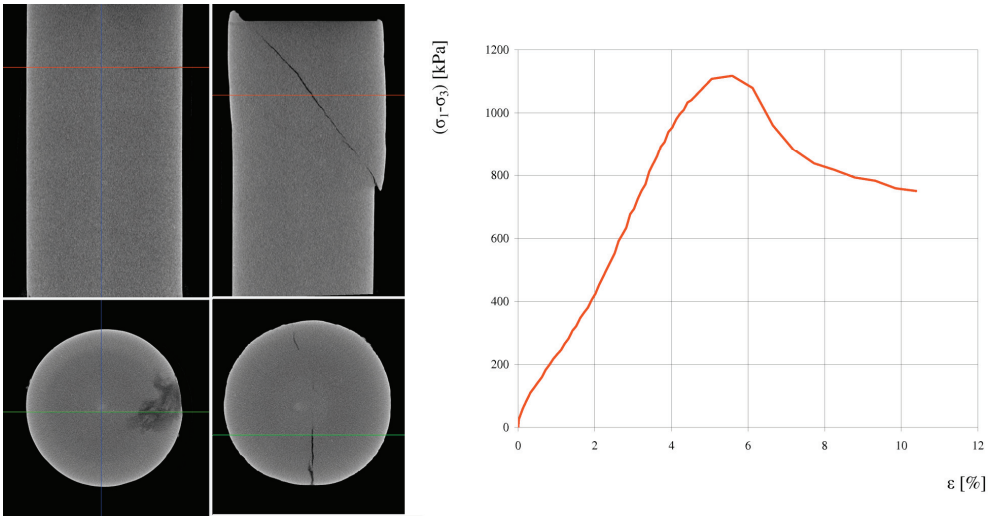

Fig. 8. Images of sample A4 before (left) and after (right) the test; stress-strain curve for σ_3 = 600 kPa

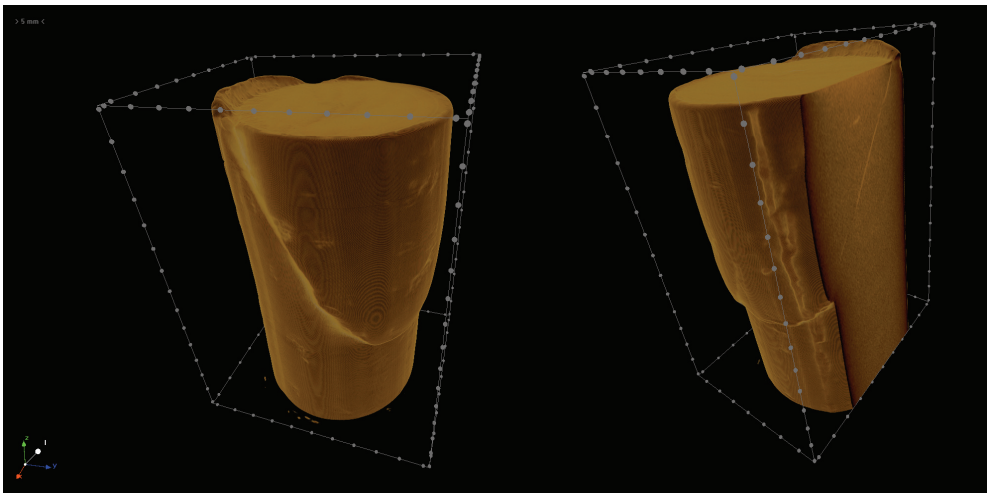

Fig. 9. 3D visualizations of sample A4

after the test. Table 3 presents estimated strength parameters (calculated with the use of the Coulomb–Mohr hypothesis). Table 4 shows gauged parameters of selected cross-sections presented in adequate figures.

Figure 14 shows the potential of basic measurements made with the research for one sample: changes in density (as a change in attenuation) and changes in surface before and after the test.

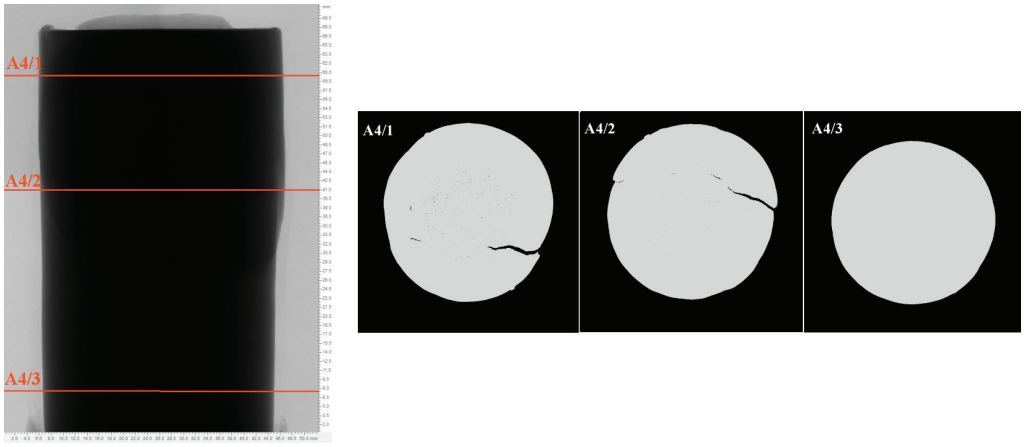

Fig. 10. Selected cross-sections of sample A4 after the triaxial test

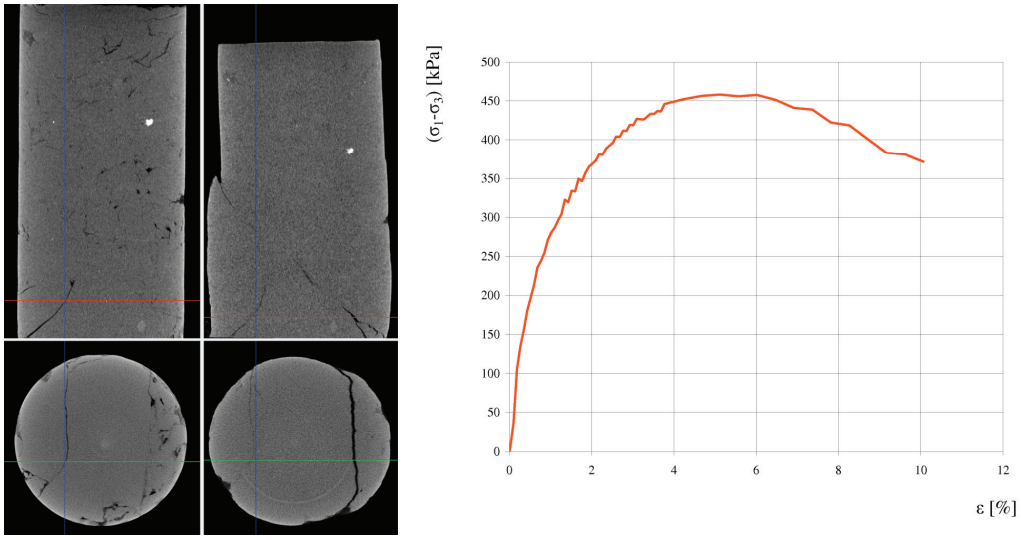

Fig. 11. Images of sample B9 before (left) and after (right) the test; stress-strain curve for σ_3 = 600 kPa)

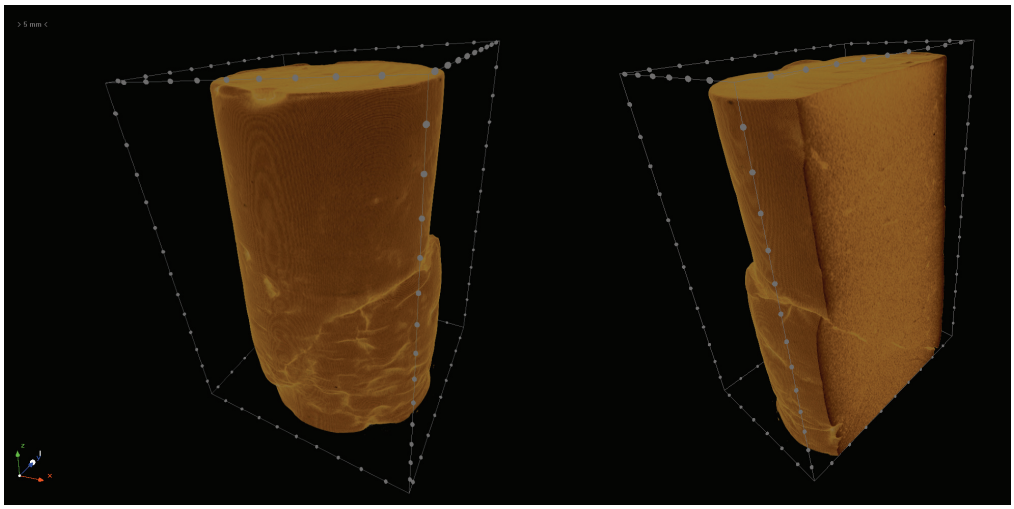

Fig. 12. 3D visualizations of sample B9 after the test

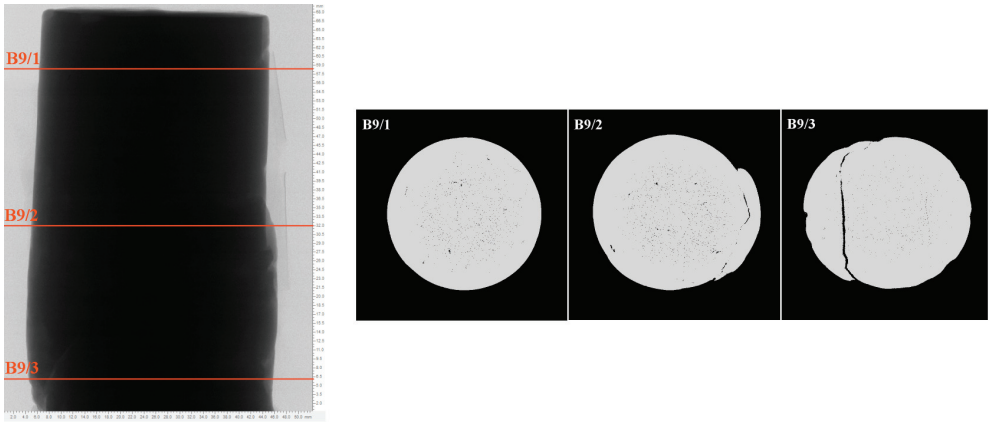

Fig. 13. Selected cross-sections of sample B9 after the triaxial test

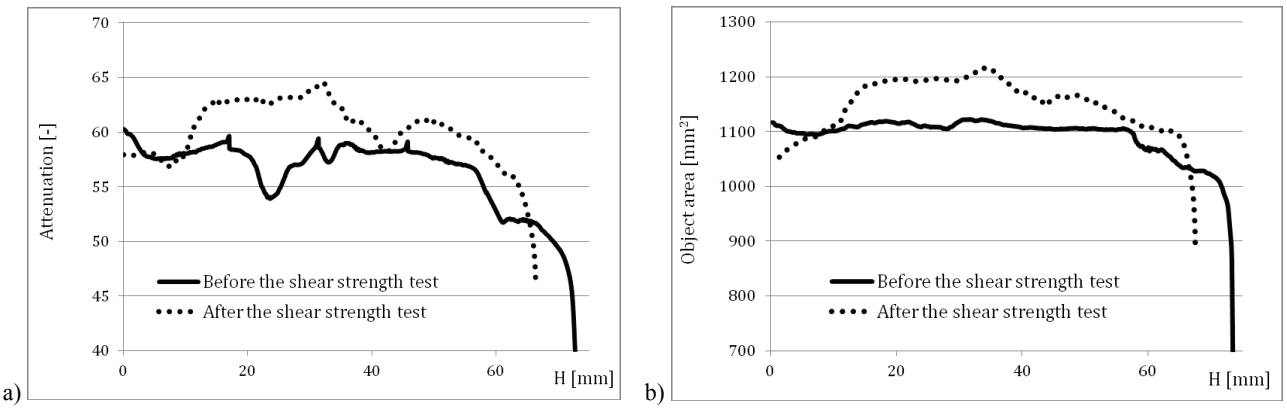

Fig. 14. The potential of basic measurements for one selected sample – A1: (a) attenuation – parameter based on Beer's law, characterizing the changes in density (as a change in attenuation); (b) surface area – changes before and after the test

The triaxial test results show that the shear strength parameters – effective cohesion c' and effective friction angle ϕ' – vary from 13.5 kPa to 22.9 kPa and from 14.0° to 33.5°, respectively. The failure criteria were generally peak strength (samples A1, A4, B9) and in one case the criterion was axial strain $\varepsilon_z = 10\%$ (sample A2). Deviatoric stress at failure varied from 1534.6 kPa for sample A1 to 457.8 kPa for sample B9. It is easy to distinguish two groups of soils: samples with greater values of deviatoric stress, i.e., A1 and A4 ($(\sigma_1 - \sigma_3)_f > 1000$ kPa), and samples with much lower values of deviatoric stress, i.e., A2 and B9 ($(\sigma_1 - \sigma_3)_f < 1000$ kPa). Such great variability in deviatoric stress values may be explained by previous cracking caused by geological stress history. The X-ray μCT scanning technology will help prove or reject this argument for individual samples.

This test allows for a non-destructive investigation of soil structure. On images from the μCT the intact sample of clayey soil appears as an almost homogeneous solid. However, when the difference between densities of constituents is sufficiently high, we can observe some differences like inclusion of organic matter (see Fig. 5), material with higher density (see Fig. 11), or visible layering (see Fig. 2). Various cracking is also well visible. If these discontinuities do not occur in the area of shear plane, they should not play an important role in soil strength. All in all, in some cases former cracking may determine the mode of failure. In the case of strongly consolidated soils taken from great depth we can observe many fissures (cracks), developed because of decompression of a specimen, or pre-fissures, connected with previous geological stress history.

In the group of selected samples pre-fissures (samples A1, B9) and cracks (A2) could be noticed, caused probably by decompression. However, in specimens A1 and A2 some cracks almost completely disappeared after the triaxial test. For sample B9, on the other hand, we could observe pre-fissures that pre-existed failure in confined compression during the test. The pre-existing fissures undoubtedly influenced the formation of shear strength, reducing the deviatoric stress value. The low value of deviatoric stress at failure was also noticed for sample A2. This soil was characterized by very low bulk density, high water,

organic matter contents and a large number of small cracks indicating strong degradation of natural soil structure. The initial condition of a specimen resulted in increasing shear strength during the confining compression test, but never reached the *in situ* value. The A4 sample did not exhibit any cracks and its structure seemed to be intact. The stress-strain curve has confirmed that.

The shear plane analysis was carried out with μCT images as well. In the case of stiff fine-grained soil taken from considerable depth, three geometric principles of the shear plane have been identified as [2]:

- Type 1 – single shear plane with an inclination $\alpha > 45°$ – the Mohr's circles analysis indicated that the failure occurred along the maximum inclination;
- Type 2 – several minor planes formed along the principal shear plane, which corresponded to either an indistinct peak or no peak in deviatoric stress,
- Type 3 – the shear plane correlated with pre-existing fissures, and strength was much lower than expected.

The test results show that for samples A1 and A4 type 1 of shear plane has occurred, connected to the high value of its peak deviatoric stress. In turn, type 3 has been determined for the B9 sample, with strength at the lowest level among all the samples analyzed. The A2 sample did not show any shear plane at the point of failure, with the contractual failure criterion (axial strain ε_z = 10%) assumed. The strength, as with the B9 sample, turned out to have been underestimated.

The images produced by the microtomography technique have three-dimensional nature, which opens the possibility of undertaking various measurements of the scanned object. The most basic properties that could be determined were the area of cross-sections, diameter and density. In the paper, 3 selected cross-sections for each specimen and their attributes are introduced (see Table 4, Figs. 4, 7, 10, 13). During standard triaxial compression, usually the axial load was measured and calculation of stress values was established based on approximated areas of speci-

Table 3. Soil strength parameters

Sample	A1	A2	A4	B9
Failure criterion	Peak deviatoric strength (indistinct)	Axial strain ε_z = 10%	Peak deviatoric strength (well pronounced)	Peak deviatoric strength (pronounced)
Deviatoric stress at failure $(\sigma_1 - \sigma_3)_f$ [kPa]	1534.6	685.2	1117.6	457.8
Effective cohesion c' [kPa]	19.0	46.7	13.5	22.9
Effective friction angle ϕ' [°]	33.5	21.4	28.7	14.0
Shear plane type [2]	Type 1	No shear plane	Type 1	Type 3

Table 4. Geometrical parameters of selected cross-sections of specimens after the TXCIU test determined from μCT scanning

Cross-section	Area [mm^2]	Area-equivalent circle diameter [mm]	Major diameter [mm]	Minor diameter [mm]
A1/1 (Fig.4)	1116.82	37.71	38.47	36.91
A1/2 (Fig.4)	1230.93	39.59	40.18	39.86
A1/3 (Fig.4)	1166.24	38.53	40.03	38.97
A2/1 (Fig.7)	1125.85	37.86	38.38	37.29
A2/2 (Fig.7)	1180.05	38.76	39.59	38.45
A2/3 (Fig.7)	1134.60	38.01	38.54	37.91
A4/1 (Fig.10)	1309.63	40.83	42.18	41.13
A4/2 (Fig.10)	1293.26	40.58	41.58	39.83
A4/3 (Fig.10)	1146.73	38.21	38.63	38.45
B9/1 (Fig.13)	1168.12	38.58	38.92	38.48
B9/2 (Fig.13)	1275.81	40.30	42.36	39.16
B9/3 (Fig.13)	1259.32	40.04	42.39	38.43

mens. It ought to be noticed that the specimens did not retain the perfect cylindrical shape after test and the differences in diameter varied. The data provided shows only a small part of the possibilities of measurements enabled by the μCT method. The method further allows other geometrical parameters of cross-sections to be evaluated, like aspect ratio and eccentricity, as well as volume of the object.

5. CONCLUSION

X-ray microtomography is a non-destructive technique of three-dimensional imaging that allows internal structure of materials to be examined. Despite not being in broad use in geotechnics, it offers new possibilities of measurement and visualization. The internal structure of soil, pore network, or various discontinuities can be recognized without destroying the specimens. In soil shear strength investigations the technique can be used for evaluation of sample quality and mode of sample failure before tests. The internal defects occurring in soil specimens as pre-existing fissures, cracks, and laminations strongly influence soil strength parameters. In some cases previous cracking may also determine the mode of failure and values of shear strength. The problem concerns especially stiff and very stiff clays taken from considerable depth.

The paper presents outcomes of an investigation into soil strength of four selected samples of clayey soils, carried out with the use of a μCT apparatus. Specimens prepared to the triaxial compression test have been scanned before and after. The shear strength parameters were estimated. The results of scanning have been presented as images of selected cross-sections and 3D visualizations of the specimens tested. They permit recognition of pre-existing fissures and influence the shear plane formed and strength parameters obtained. In addition, some changes in the shape and area for selected cross-sections of samples following the confining compression tests have been determined.

The present examination is preliminary and further investigations are planned. However, the results obtained clearly show the usefulness and potential of microtomography for geotechnical applications. The main advantage of μCT scanning is that the specimens can be examined without changes made to their significant properties. This visualization technique may increase our comprehension of mechanical behavior of soils and certainty of estimated strength parameters. It can help with proper analysis of strength tests and enables the selection of appropriate soil samples for testing.

REFERENCES

[1] FLANNERY B.P., DECKMAN H.W., ROBERGE W.G., D'AMICO K.L., *Three-dimensional x-ray microtomography*, Science, 1987, 237.

[2] GASPARRE A., *Advanced laboratory characterization of London clay*, PhD thesis, 2005.

[3] GREGOR T. et al., *Correlating Micro-CT Imaging with Quantitative Histology*, Injury and Skeletal Biomechanics, 2012.

[4] HALL S.A., BORNERT M., DESRUES J., PANNIER Y., LENOIR N., VIGGIANI G., BESUELLE P., *Discrete and continuum analysis of localised deformation in sand using X-ray _CT and volumetric digital image correlation*, Geotechnique, 2010, 60, No. 5.

[5] HEAD K.H., *Manual of Soil Laboratory Testing*, 1986, Vol. 3.

[6] HEIJS A.W.J., DE LANGE J., *Determination of pore networks and water content distributions from 3-D computed tomography images of a clay soil*, Bioimaging, 1997, 5.

[7] KETCHAM R.A., CARLTON W.D., *Acquisition, optimization and interpretation of X-ray computed tomographic imagery: applications to the geosciences*, Computers & Geosciences, 2001, 27.

[8] LU S., LANDIS E.N., KEANE D.T., *X-ray microtomographic studies of pore structure and permeability in Portland cement concrete*, Materials and Structures, 2006, 39.

[9] PIRES L.F., BORGES J.A.R., BACCHI O.O.S, REICHARDT K., *Twenty-five years of computed tomography in soil physics: A literature review of the Brazilian contribution*, Soil & Tillage Research, 2010, 110.

[10] PN-EN ISO 14688, Geotechnical investigation and testing – Identification and classification of soil.

[11] SkyScan1172, Desktop X-ray microtomograph, Instruction Manual, 2005.

[12] TAUD H., MARTINEZ-ANGELES R., PARROT J.F., HERNANDEZ--ESCOBEDO L., *Porosity estimation method by X-ray computed tomography*, Journal of Petroleum Science and Engineering, 2005, 47.

[13] WILDENSCHILDA D., HOPMANS J.W., VAZ C.M.P, RIVERS M.L., RIKARD D., CHRISTENSEN B.S.B., *Using X-ray computed tomography in hydrology: systems, resolutions, and limitations*, Journal of Hydrology, 2002, 267.

[14] WONG R.C.K., *Strength of two structured soils in triaxial compression*, International Journal for Numerical and Analytical Methods in Geomechanics, 2001, 25.

[15] VIGGIANI G., LENOIR N., BESUELLE P., DI MICHIEL M., MARELLO S., DESRUES J., KRETZSCHMER M., *X-ray microtomography for studying localized deformation in fine-grained geomaterials under triaxial compression*, C. R. Mecanique, 2004, 332.